

RF DESIGN OF THE IFMIF-EVEDA RFQ

F. Grespan, A. Palmieri, A. Pisent INFN/LNL, Legnaro (PD) Italy

Abstract

The RFQ of IFMIF-EVEDA project is characterized by very challenging specifications, with 125 mA of deuteron current accelerated up to 5 MeV. Upon beam dynamics studies, it has been chosen a law for the variation of R_0 and voltage along the structure; this law provides a significant reduction in terms of structure length, beam losses and rf power consumption. Starting from these outcomes, the rf study of the RFQ, aimed at determining the optimum design of the cavity shape, was performed. The stabilization issues were also addressed, through the analysis of the RFQ sensitivity to geometrical errors, by means of perturbative theory-based algorithms developed for this purpose. Moreover the determination of the main 3D details of the structure was also carried out. In this article the results of the rf studies concerning the above-mentioned topics are outlined.

RFQ PARAMETERS AND CAVITY DESIGN

The main RFQ parameters are listed in Table 1, and the 3D layout in Figure 1.

Table 1: IFMIF RFQ Input Design Parameters

Particles	D+	
Frequency	175	MHz
Input Current	130	mA
Energy (in-out)	0.1-5	MeV
Max Surface Field	25.2	MV/m (1.8 Kp)
Length L	9.78	m
Voltage min/max	79/132	kV
Mean aperture R_0	4.1 / 7.1	mm
Pole tip radius ρ	3.08/5.33	mm

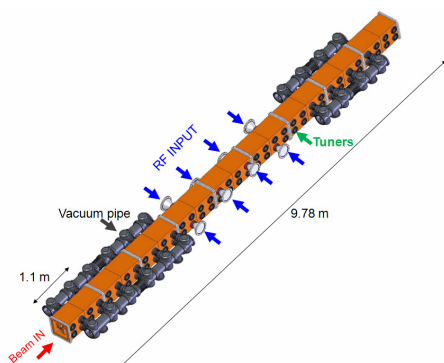


Figure 1: IFMIF RFQ schematic layout.

The IFMIF EVEDA RFQ beam dynamics study[1] was aimed at minimizing beam losses at high energy, reducing

the RFQ length and power consumption. A closed-form and continuous up to the 2nd derivative voltage law $V(z)$ was used. In this way it is possible to increase the voltage smoothly along the accelerator part and to have continuous cut-off frequency variations.

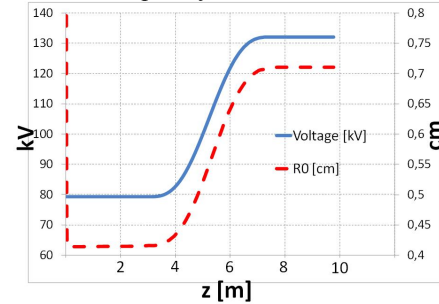


Figure 2: Mean aperture and voltage profile along the RFQ.

The goal of the cavity design was the optimization of the transverse section in order to match the local cut-off frequency with respect to local TE_{21} cut-off frequency $f(z)$ variation due both to voltage and aperture variation, by varying the Vane Base Width $2 \cdot W_1$ along the RFQ with the usage of the RFQFISH routine. The minimum W value (1 cm) was chosen in order to allow cooling channel positioning and the maximum W_1 value (1.5 cm) to avoid mechanical oscillations during machining. The upper flat surfaces H_1 and H_2 (9 cm) allow the positioning of tuners and RF couplers (Fig.3). Moreover the choice of the section was also dictated by the fact that a “square” shape of the RFQ cross-section allows, for a given frequency and R_0 , a better volume/surface ratio and a subsequent Q improvement (about 10%) with respect to a “triangular” shape.

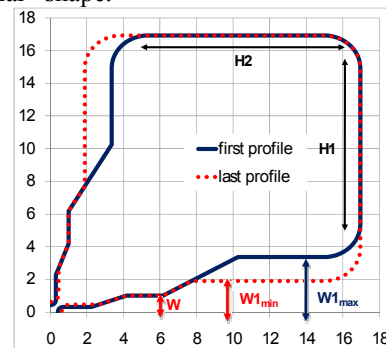


Figure 3: The variable shape of the RFQ section.

The main parameters obtained from the SUPERFISH optimization are summarized in Table 2.

Table 2: SUPERFISH Results

Q ₀ (SF) (z=0-z=L)	15100-16700	
2D Power (SF)	450	kW
Stored Energy	6.6	J
Max H field (z=0-z=L)	3000-4500	A/m
Max. Power Density (z=0-z=L)	1.6-3.1	W/cm ²
Total power P _d	1.345	MW

The P_d is related to the 2D power calculated by SUPERFISH, P_{SF}, by means of the relationship

$$P_d = P_{SF} \alpha_{3D} \alpha_v + P_b$$

where $\alpha_{3D}=1.3$ (for 3D losses), P_b is the beam power at 130 mA and $\alpha_v = 1.21$ ($= 1.1^2$) for Voltage enhancement. The sensitivity with respect to geometrical errors was addressed both numerically and analytically, and it was found that the maximum [minimum] sensitivity χ is located in the initial [final] section of the RFQ, where $\Delta f/\Delta R_0=11.8$ MHz/mm [7.5 MHz/mm].

FIELD STABILIZATION ISSUES

Geometrical errors in the RFQ section produce perturbations on the nominal voltage profile $U_0(z)$ via capacitance perturbations. General beam dynamics considerations prescribe that $|\Delta U(z)/U_0(z)| < 0.01$ and $|U_{qd1,qd2}(z)/U_0(z)| < 0.02$ [2] where $\Delta U(z)$ and $U_{qd1,qd2}(z)$ are the voltage perturbations due to upper quadrupole modes and the two kinds of dipole modes respectively. In order to reach such goal, it is necessary to use a system of N_T slug tuners per quadrant of radius a and depth h variable in the interval $[0, h_{max}]$. Each tuner can vary the resonant frequency of the RFQ of an amount equal to $\Delta f_i = \chi_i h$, χ_i being the tuner sensitivity related to the magnetic field on the upper RFQ wall. The idea is that the tuning range (the frequency interval that can spanned by the tuners) $\Delta f_{TR} = 2N_T \chi_i h_{max}$ should be able to correct for frequency shifts induced by geometrical error Δf_q with appropriate margin, that is $\Delta f_{TR} = k \Delta f_q$ with $k > 1$. If f_c is the average cut-off frequency of the RFQ and f_0 is the operating frequency, the tuning range is symmetric around f_0 , in the sense that $\Delta f_{TR} = f_0 - f_c$. If all tuners, couplers and vacuum ports are placed along, say, H1 surface, then the number of tuners is determined by the space constraints. Looking at the structure of IFMIF RFQ (Figure 1), there are $N_T=22$ longitudinal locations per quadrant available for tuners. However, N_T can be increased to 24 or 27, by placing the tuners in H2 surface and all the other ancillaries along H1 (see Figure 3), thus permitting the tuners to be periodically spaced. In the following the effectiveness of tuning will be discussed by comparing the case of coupled and uncoupled RFQs in terms of tuning range required, with the coupling element is located at $L/2$. For simplicity let us assume that the

RFQ is uniform with $R_0=4.1$ mm, $a=45$ mm and $\chi_i=800$ Hz/mm. In order to understand better the meaning of the tuning range, let us suppose to have a geometric perturbation $\Delta R_0=0.04$ mm if $0 < z < L/2$ and $\Delta R_0=0$ mm otherwise and equal in all the four quadrants. ($\Delta U(z) \neq 0$, $U_{qd1,qd2}(z)=0$). For this kind of perturbation, we have a local frequency variation equal to 500 kHz. The corresponding $\Delta U(z)/U_0(z)$ functions for the case of coupled and uncoupled RFQ are shown in Figure 5. Now, let us suppose that our tuning system is rated for $\Delta f_{TR} = 1$ MHz corresponding to $h_{max}=28.6$ mm and $k=2$. It is possible to show that, in this case, the voltage variation can be reduced to $\pm 1.5\%$ in one tuning step without exploiting the whole tuners depth capability, both for coupled and uncoupled RFQ's (Figures 4 and 5).

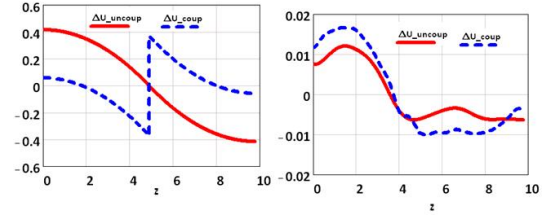


Figure 4: The $\Delta U/U_0$ function before (left) and after (right) one tuning step.

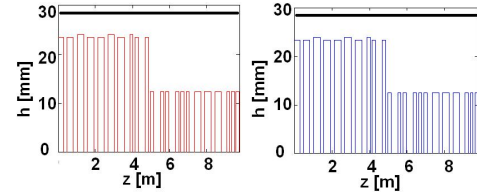


Figure 5: The tuner depths needed for the uncoupled (left) and coupled (right) case vs. tuner locations.

The situation is different if the tuning range is such that $k=1$. In fact, in this case, the tuning range is halved, and therefore all tuner depths saturate to $h_{max}=14.3$ mm in the first half of the RFQ and the voltage variation does not reduce less than 7.5% for the coupled case and 8.8 % for the uncoupled case. In conclusion, for our L/λ ratio, the usage of a coupling element does not reduce significantly the tuning range needed and the chosen tuning range seems to be effective to contrast perturbations also with an unsegmented structure. This is somewhat in agreement with the fact that the SNS RFQ (which is only 15% shorter than IFMIF RFQ in terms of L/λ) does not use any coupling cell.

As for the dipoles, the minimum sensitivity to dipole errors vs. boundary conditions for coupled and uncoupled structures is substantially the same. This can be shown by comparing in both cases the minimum value of the quantity h_{dip} as a function of the voltage slope $s_a = U'_{qd1,d2}(0)/U_{qd1,d2}(0)$ (boundary condition) at the beginning of the RFQ [6]. Such quantity is defined as the maximum value with respect to z and z_0 of

$U_{qd1,d2}(z)/U_0(z)$ in the case of a delta capacitance perturbation located in $z=z_0$ (Figure 6).

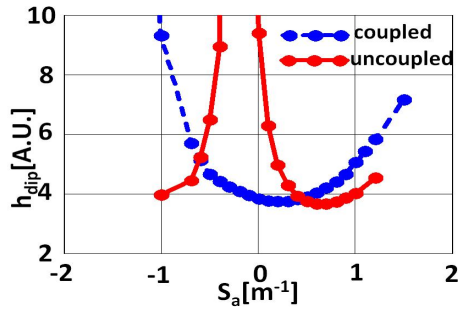


Figure 6: h_{dip} comparison for IFMIF RFQ.

The tuning system effectiveness will be experimentally tested on a real-scale aluminium model of the RFQ, which will allow also the possibility of introducing a coupling element in between.

3D MODELING OF THE RFQ AND RELATED HFSS SIMULATIONS

The study of the 3D details of the RFQ, performed with the code HFSS v. 11.1 was concentrated mainly on the following aspects: voltage law validation, end cell design and study of the vacuum grid. In the following the power densities are calculated by using the $\alpha_{3D}\alpha_v$ margins defined before.

The validation of the voltage law was made by comparing the magnitude of the electric fields in a point $(X_0, Y_0) = (1\text{cm}, 1\text{cm})$ along the symmetry axis of the quadrant given by SUPERFISH and HFSS. The agreement between the two field profiles is within 4% and the Q value calculated by HFSS is equal to 15400. Moreover, it was also possible to calculate the value of the longitudinal surface currents that are non vanishing, since the voltage profile is not constant. This component intercepts discontinuities due to modularity of RFQ, but its value ($\sim 4\text{ A/m}$) is negligible respect to the transverse component ($\sim 2000\text{ A/m}$).

The design of the end cells was accomplished too, by determining the dimensions of the vane undercuts that assure the achievement of the proper boundary conditions at the RFQ extremities. For such structure, the power density was checked in view of the 3D thermo-structural calculation. In Figure 7 the geometry of the matched Low Energy undercut is shown, as well as the power density profile.

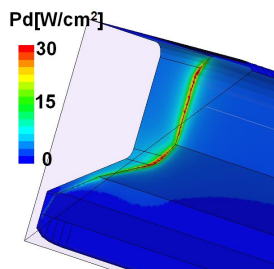


Figure 7: Power density profile along the end-cell.

As for the vacuum grids, they introduce a discontinuity in the upper wall of the RFQ, that creates a frequency shift and an enhancement in current density. In order to understand the amount of such effects, simulations on a 27.5 cm RFQ slice were performed for the grid model of Figure 8, in which the slit distance δ was varied. The results are summarized in Table 3 and Figure 9.

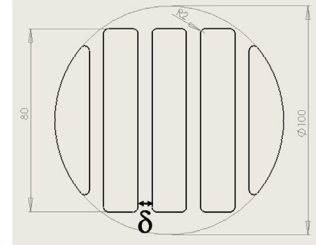


Figure 8: The vacuum grid model.

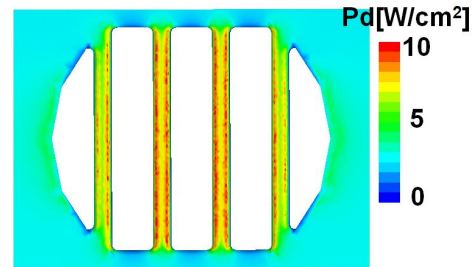


Figure 9: Power density in the vacuum grid for $\delta=6.5$ mm.

Table 3: Vacuum Grid Main Parameters

case	δ [mm]	f[MHz]	Pd grid [W]
nominal	No grid	174.375	153 (on the flat surface to be occupied by the grid)
1	6.25	174.245	186
2	7.25	174.267	187
3	8.25	174.289	188
4	9.25	174.312	179

The Q drop due to the vacuum grid keeps under 1% and the power density enhancement due to the grid is about 3 with respect to the flush wall. The validation of the current layout of the grid will be given upon thermal simulations whose input data are the above calculated power densities.

REFERENCES

- [1] M. Comunian, et. al. " Beam Dynamics of the IFMIF-EVEDA RFQ", EPAC 2006, Genoa (Italy).
- [2] M. Comunian, et. al. this conference.
- [3] A. Pisent, et. al. " IFMIF-EVEDA RFQ Design", EPAC 2006, Genoa (Italy).
- [4] A. Ratti et al, Proc. LINAC98, Chicago, (USA), August 1998, p. 276.
- [5] A. Pisent et al. "The TRASCO-SPES RFQ" LINAC 2004 conference, Lübeck (Germany).
- [6] A. France, LNL colloquium 16 July 2007.